



## Modeling Human Protein Aggregation Cardiomyopathy Using Murine Induced Pluripotent Stem Cells

PATTRARANE LIMPHONG,<sup>a,\*</sup> HUALI ZHANG,<sup>a,\*</sup> ELISABETH CHRISTIANS,<sup>a</sup> QIANG LIU,<sup>a</sup> MICHAEL RIEDEL,<sup>a</sup>  
KATHRYN IVEY,<sup>b</sup> PAUL CHENG,<sup>b</sup> KATIE MITZELFELT,<sup>a</sup> GRAYDON TAYLOR,<sup>a</sup> DENNIS WINGE,<sup>c,d</sup>  
DEEPAK SRIVASTAVA,<sup>b</sup> IVOR BENJAMIN<sup>a,d</sup>

**Key Words.** Induced pluripotent stem cells • Cardiomyocytes •  $\alpha$ B-Crystallin (CryAB) • Protein aggregation • Cardiac hypertrophy

### ABSTRACT

Several mutations in  $\alpha$ B-crystallin (CryAB), a heat shock protein with chaperone-like activities, are causally linked to skeletal and cardiac myopathies in humans. To better understand the underlying pathogenic mechanisms, we had previously generated transgenic (TG) mice expressing R120GCryAB, which recapitulated distinguishing features of the myopathic disorder (e.g., protein aggregates, hypertrophic cardiomyopathy). To determine whether induced pluripotent stem cell (iPSC)-derived cardiomyocytes, a new experimental approach for human disease modeling, would be relevant to aggregation-prone disorders, we decided to exploit the existing transgenic mouse model to derive iPSCs from tail tip fibroblasts. Several iPSC lines were generated from TG and non-TG mice and validated for pluripotency. TG iPSC-derived cardiomyocytes contained perinuclear aggregates positive for CryAB staining, whereas CryAB protein accumulated in both detergent-soluble and insoluble fractions. iPSC-derived cardiomyocytes identified by cardiac troponin T staining were significantly larger when expressing R120GCryAB at a high level in comparison with TG low expressor or non-TG cells. Expression of fetal genes such as atrial natriuretic factor, B-type natriuretic peptide, and  $\alpha$ -skeletal  $\alpha$ -actin, assessed by quantitative reverse transcription-polymerase chain reaction, were increased in TG cardiomyocytes compared with non-TG, indicating the activation of the hypertrophic genetic program in vitro. Our study demonstrates for the first time that differentiation of R120G iPSCs into cardiomyocytes causes protein aggregation and cellular hypertrophy, recapitulating in vitro key pathogenic hallmarks found in both animal models and patients. Our findings pave the way for further studies exploiting this cell model system for mechanistic and therapeutic investigations. *STEM CELLS TRANSLATIONAL MEDICINE* 2013;2:161–166

### INTRODUCTION

$\alpha$ B-crystallin (CryAB), a small heat shock protein, functions as a chaperone for several client proteins, including the intermediate filament protein desmin, thereby preserving skeletal and cardiac muscle cell organization and function [1]. R120G mutation in human CryAB is responsible for an autosomal-dominant, multisystem disorder affecting eye lens and skeletal muscle and causing clinical and/or pathological signs of cardiomyopathy [2]. Transgenic mice expressing R120GCryAB specifically in cardiomyocytes show signs of dilated cardiomyopathy and developed heart failure as early as 6–7 months, depending on the level of expression [3, 4].

The R120G mutation corresponds to the loss of CryAB chaperone function and is character-

ized by the formation of large cytoplasmic aggregates. The R120G mutation is also a “gain of toxic” function likely mediated by new, possibly illegitimate protein-protein interactions and the formation of soluble (preamyloid) oligomers [5, 6].

Induced pluripotent stem cells (iPSCs) can be derived from various cell types and differentiated in beating cardiomyocytes. The arrhythmogenic long-QT, Timothy, and LEOPARD syndromes were recapitulated in iPSC-derived cardiomyocytes (iCMs) from patients, providing proof-of-concept for generating disease-specific cardiomyocytes [7–9].

In this brief report, we describe our attempt to model protein aggregation cardiomyopathy using mouse iCMs, mimicking properties found in patients and mouse models. This first step, which was achieved with our transgenic model,

<sup>a</sup>Division of Cardiology,  
<sup>c</sup>Division of Hematology, and  
<sup>d</sup>Department of  
Biochemistry, University of  
Utah School of Medicine, Salt  
Lake City, Utah, USA;  
<sup>b</sup>Gladstone Institute of  
Cardiovascular Disease, San  
Francisco, California, USA

\*Contributed equally as first  
authors.

Correspondence: Ivor Benjamin,  
M.D., Departments of Internal  
Medicine and Biochemistry, 30  
North 1900 East, Room 4A100,  
Salt Lake City, Utah 84132, USA.  
Telephone: 801-581-6785; Fax:  
801-585-1082; E-Mail:  
ivor.benjamin@hsc.utah.edu

Received June 11, 2012;  
accepted for publication  
December 7, 2012; first  
published online in *SCTM*  
*EXPRESS* February 19, 2013.

©AlphaMed Press  
1066-5099/2013/\$20.00/0

[http://dx.doi.org/  
10.5966/sctm.2012-0073](http://dx.doi.org/10.5966/sctm.2012-0073)

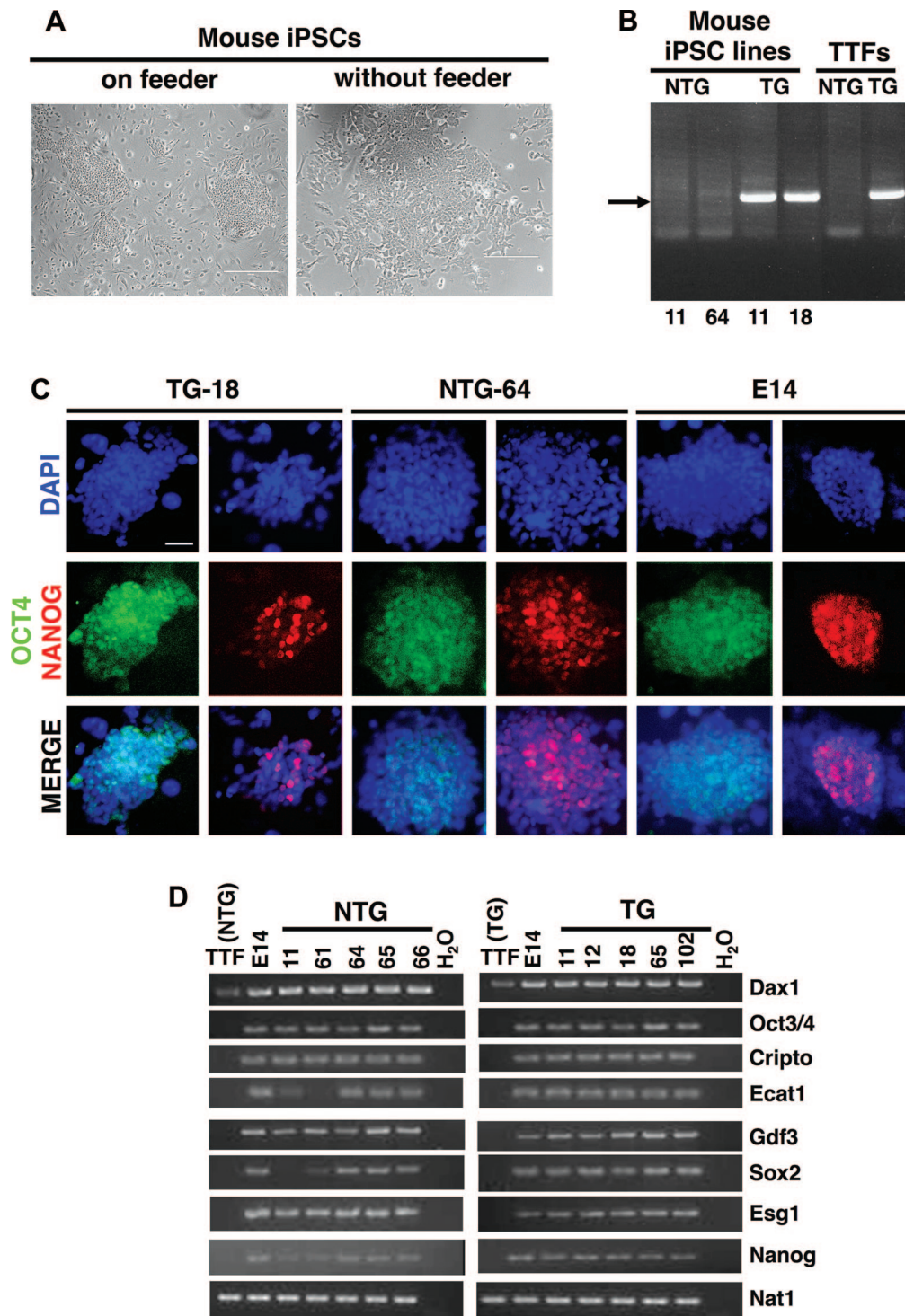


**Figure 1.** Generation of NTG and TG (R120G  $\alpha$ B-crystallin [CryAB]) mouse iPSCs. **(A):** Morphologies of mouse iPSCs in SNL feeder and feeder-independent cultures. Scale bars = 400  $\mu$ m (left), 200  $\mu$ m (right). **(B):** Genotyping of induced pluripotent stem colonies from NTG-11, NTG-64, TG-11, and TG-18 along with NTG-TTFs and TG-TTFs used as controls. Arrow indicates the amplified polymerase chain reaction (PCR) product in transgenic samples. **(C):** Immunofluorescence staining of pluripotent markers OCT4 (green) and NANOG (red) in representative iPSC and embryonic stem (ES) cell (E14, mouse embryonic stem cells) clones. An inverted fluorescent microscope was used to image the samples, and pictures were equally treated using autocontrast enhancement. Scale bar = 100  $\mu$ m. **(D):** Reverse transcription-PCR analysis of embryonic stem cell marker genes in mouse iPSCs, E14, and TTFs. We used primers that amplified endogenous but not transgenic transcripts. (A full list of abbreviations is given in the supplemental online data.) Abbreviations: DAPI, 4',6-diamidino-2-phenylindole; iPSC, induced pluripotent stem cell; NTG, nontransgenic; TG, transgenic; TTF, tail tip fibroblast.

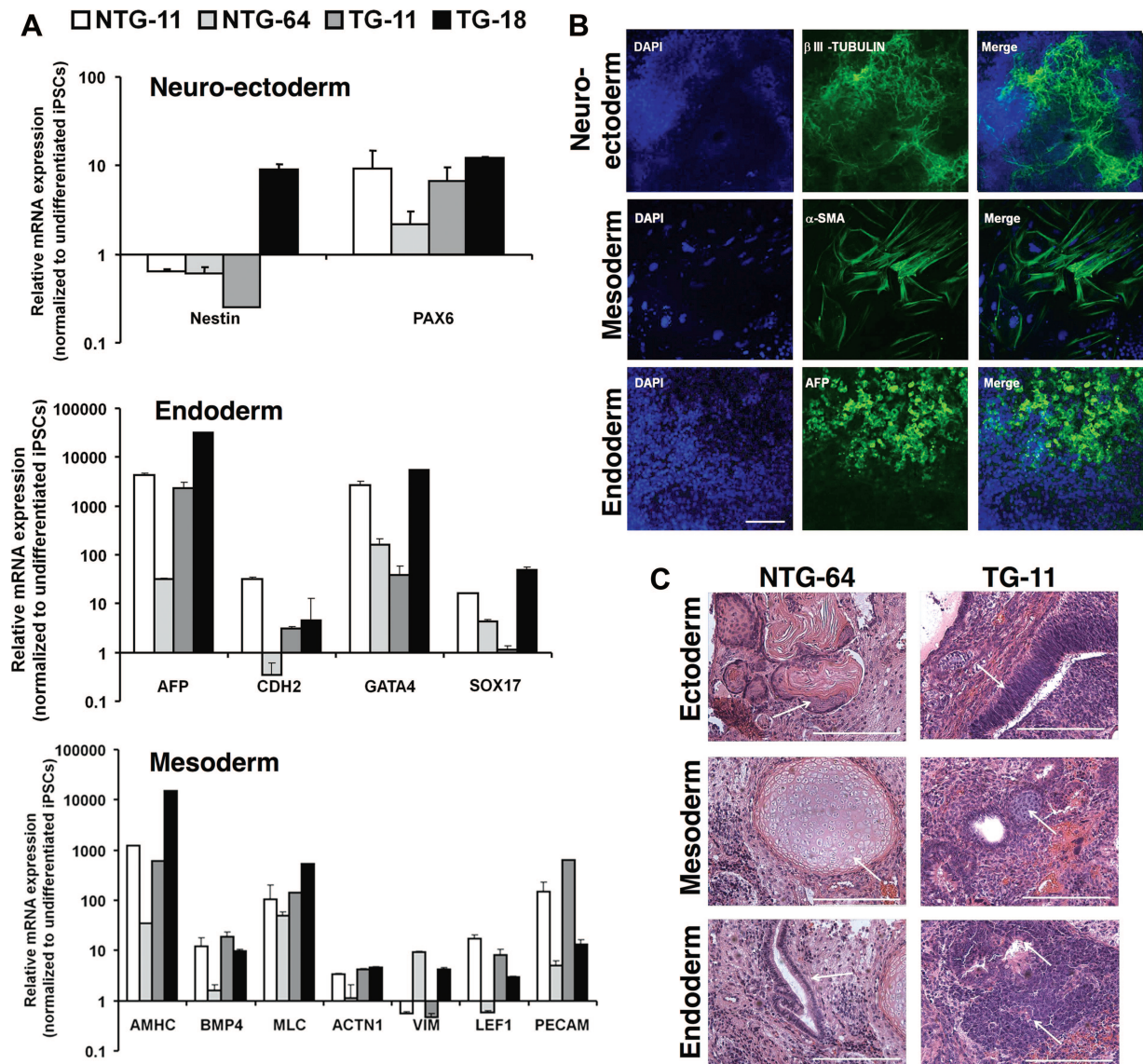


**Figure 2.** In vitro embryoid bodies (EBs) mediated differentiation of NTG and TG iPSCs. **(A):** Differentiated NTG and TG EBs were analyzed by quantitative polymerase chain reaction to detect ectoderm, endoderm, and mesoderm marker expression. Graphs show relative expression to undifferentiated iPSCs in the corresponding sample. **(B):** iPSCs were stained  $\beta$ III-tubulin (neuroectoderm),  $\alpha$ -SMA (mesoderm), and AFP (endoderm). A fluorescence microscope was used to image the samples, and representative pictures are from a differentiated TG-11 line. Scale bar = 50  $\mu$ m. **(C):** Teratoma sections derived from representative NTG-64 and TG-11 iPSCs were collected after 6 weeks, and sections were stained with hematoxylin and eosin. Teratomas contained representative tissues of the three germ layers: pluristratified epithelium (ectoderm), cartilage (mesoderm), and columnar epithelium (endoderm). Scale bars = 50  $\mu$ m. (A full list of abbreviations is given in the supplemental online data.) Abbreviations: BMP, bone morphogenetic protein; DAPI, 4',6-diamidino-2-phenylindole; iPSC, induced pluripotent stem cell; NTG, nontransgenic;  $\alpha$ -SMA,  $\alpha$ -smooth muscle actin; TG, transgenic.

supports ongoing efforts to establish the pathogenic role of cardiac aberrant protein aggregation in similar human systems.

## MATERIALS AND METHODS

An expanded Materials and Methods section is available in the supplemental online data.

## RESULTS

To generate iPSCs, we used tail-tip fibroblasts from one transgenic (TG) male harboring  $\alpha$ -MHC-R120GCryAB and one non-TG

(NTG) male and reprogrammed them by infection with retrovirus containing the following four factors: Oct4, Klf4, Sox2, and Myc. Both NTG and TG iPSC clones possessed embryonic stem (ES) cell-like morphology (Fig. 1A) and were correctly re-genotyped (Fig. 1B). Immunodetection of NANOG and OCT3/4 proteins (Fig. 1C; supplemental online Fig. 1) and reverse transcription-polymerase chain reaction carried out for several ES cell marker genes (Fig. 1D; supplemental online Table 1) demonstrated that our mouse iPSCs expressed pluripotent genes similar to those of mouse ES cells (E14). Further experiments were performed on NTG ( $n = 5$ ) and TG ( $n = 5$ ) iPSC lines before focusing on lines 64 (NTG) and 11 (TG), which were shown to have a normal karyotype with 40 acrocentric



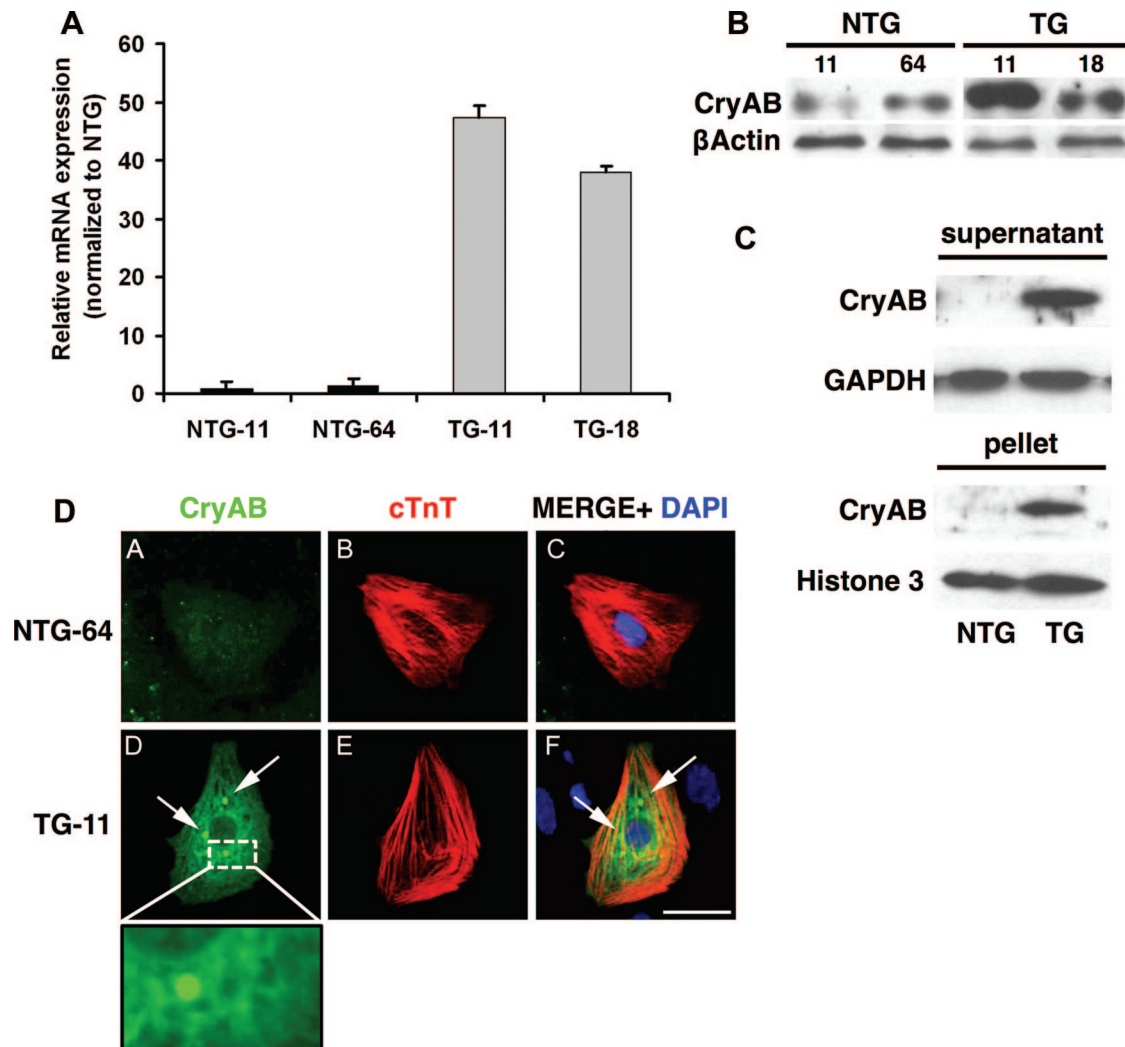


**Figure 3.** CryAB expression and aggregation in differentiated cardiomyocytes produced in TG EBs. **(A):** Quantitative polymerase chain reaction analysis of CryAB in NTG-11, NTG-64, TG-11, and TG-18 differentiated induced pluripotent stem cells (iPSCs) compared with undifferentiated iPSCs. **(B):** Western blots (EB total extract) show CryAB protein expression in EBs derived from NTG and TG iPSCs. **(C):** Western blots of the detergent-soluble (supernatant) or insoluble (pellet) fractions of EBs show partial accumulation of CryAB protein into the insoluble fraction in TG samples. GAPDH and Histone H3 were used as the loading controls. **(D):** cTnT immunostaining was used to identify cardiomyocytes in differentiated replated EBs. Only cardiomyocytes derived from TG iPSCs displayed perinuclear protein aggregates (arrows, inset: high-magnification view of perinuclear region). Shown are CryAB (green), cTnT (red), and DAPI (blue) in representative NTG-64 and TG-11. Scale bar = 50  $\mu$ m. (A full list of abbreviations is given in the supplemental online data.) Abbreviations: CryAB,  $\alpha$ B-crystallin; cTnT, cardiac troponin T; DAPI, 4',6-diamidino-2-phenylindole; NTG, nontransgenic; TG, transgenic.

chromosomes (supplemental online Fig. 2; supplemental online Table 2).

To determine NTG and TG iPSCs' differentiation capacity, floating embryoid bodies (EBs) were generated and then shown by quantitative polymerase chain reaction to have up-regulated markers for all three germ layers (Fig. 2A). This was further confirmed by positive immunodetection of  $\beta$ -III-tubulin,  $\alpha$ -smooth muscle actin ( $\alpha$ -SMA), and  $\alpha$ -fetoprotein (AFP) (Fig. 2B). Differentiated EBs showed spontaneous beating areas starting around day 7 (supplemental online Movies 1A and 1B). To assess pluripotency *in vivo*, NOD-SCID mice were injected with iPSCs, and teratomas harvested after 6–8 weeks contained cell types representative of the three germ layers (Fig. 2C).

Accumulation of insoluble CryAB aggregates in the cytoplasm and cardiac hypertrophy are major characteristics of

R120GCryAB cardiomyopathy in mice [4]. Since R120GCryAB is under the control of the cardiac-specific  $\alpha$ -MHC in TG iPSCs, the mutant protein is expressed only in cells committed to cardiac lineage. After 12 days of differentiation, EBs from TG iPSCs exhibited markedly increased levels of CryAB mRNA and protein (Fig. 3A, 3B). Following cellular protein fractionation, the R120GCryAB level was found in both detergent-soluble and insoluble fractions in EBs from TG iPSCs (Fig. 3C). In contrast, NTG EBs contained a much lower amount of CryAB, corresponding to the endogenous level of expression, detectable only after longer exposure of Western blot (data not shown).

To reveal aggregates in iCMs, EBs were collected after 12 days, and cells were stained using the cardiac-specific marker troponin T (cTnT) to identify the iCMs and colabeled with CryAB

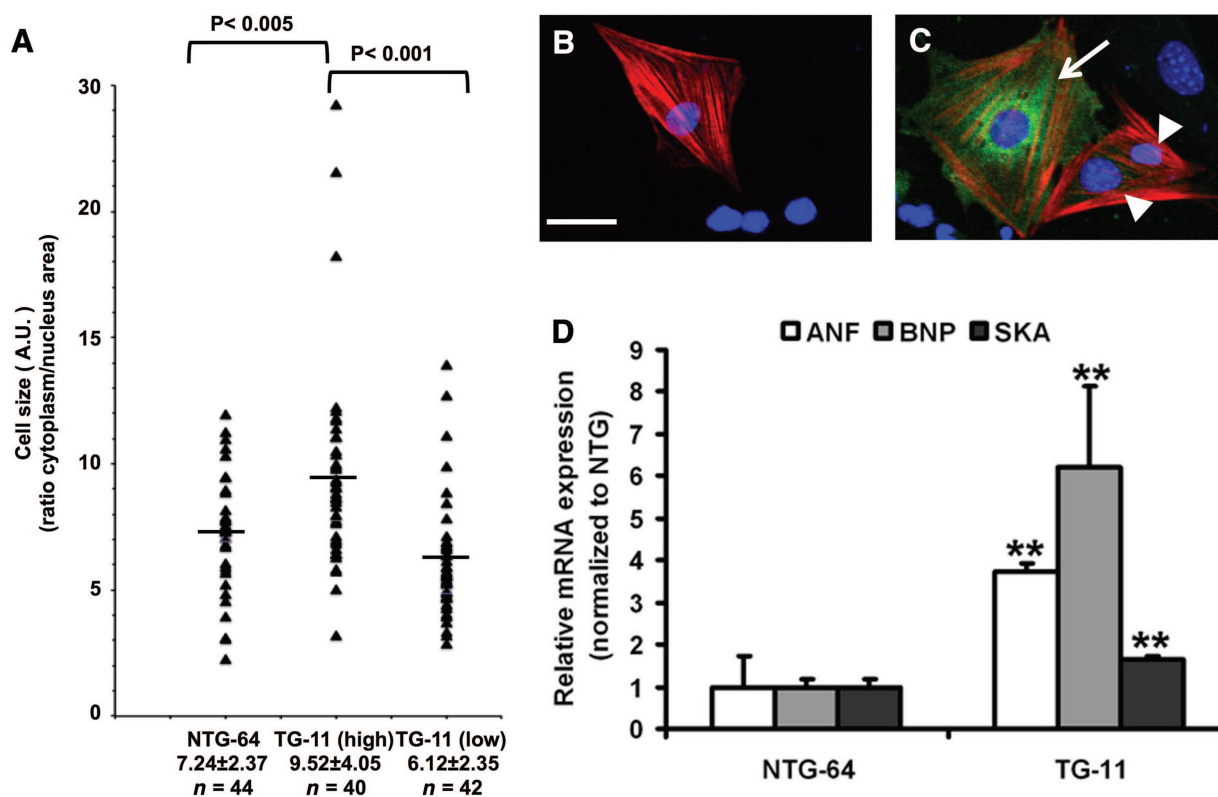


**Figure 4.** Cardiomyocytes derived from R120G  $\alpha$ B-crystallin (CryAB) TG induced pluripotent stem cells (iPSCs) show hypertrophic features. (A–C): Thirty days after EB differentiation, cells from beating NTG-64 and TG-11 samples were dissociated, replated, and stained ([B, C] as in Fig. 3D). (A): Cell and nucleus surface of cardiac troponin T (cTnT)-positive cardiomyocytes of representative NTG-64 and TG-11 lines were measured using ImageJ, and relative values are shown in the graph with an indication of the mean relative value (horizontal line). (B, C): Cardiomyocytes derived from NTG and TG iPSC were stained for cTnT and CryAB. (B): NTG iPSC-derived cardiomyocytes (iCMs) had a very low and therefore barely detectable level of CryAB. (C): CryAB staining of TG iCMs revealed two populations of cells with high and low levels of expression. Scale bar = 50  $\mu$ m. (D): Quantitative polymerase chain reaction analysis of hypertrophy gene markers such as ANF, BNP, and SKA revealed a significant increase in TG-11 fluorescence-activated cell sorting (FACS)-enriched cardiomyocytes compared with NTG-64 FACS-enriched cardiomyocytes. The cardiomyocytes used for the quantitative PCR analysis experiment contained approximately 60% cardiomyocyte purity. Data are represented as mean  $\pm$  SD.  $n = 3$ ; \*\*,  $p < .05$  (Student's  $t$  test). (A full list of abbreviations is given in the supplemental online data.) Abbreviations: A.U., arbitrary units; ANF, atrial natriuretic factor; BNP, B-type natriuretic peptide; NTG, nontransgenic; SKA,  $\alpha$ -skeletal  $\alpha$ -actin; TG, transgenic.

antibodies to decorate the aggregates. A representative example of an iCM with a high level of CryAB expression and the presence of perinuclear aggregates is shown in Figure 3D. Approximately 57% of TG iCMs contained aggregation (data not shown).

To monitor the size of iCMs, beating EBs were dissociated and replated after 30 days [7]. Cells were stained to identify the cTnT-positive cardiomyocytes and to detect CryAB expression. A careful examination of TG iCMs revealed two populations of cells, which we arbitrarily classified as high and low expressors (Fig. 4A, 4C). As previously indicated, the NTG cells expressed a low-endogenous level of CryAB (Figs. 3D, 4B). To circumvent any bias, cell surface areas were measured using a computerized morphometric system (ImageJ software, NIH) and were expressed as a ratio relative to the nucleus surface. Our results indicate that the TG iCMs (high expressors) were significantly larger than the TG low expressors or the NTG ones (55% and 25%, respectively,  $p < .05$ ) (Fig. 4A).

Since cardiac hypertrophy triggers the re-expression of fetal genes, we next determined whether mouse R120G CryAB iCMs could exhibit such reprogramming of gene expression. To obtain samples enriched in cardiomyocytes, EB cells (day 30) were stained with tetramethylrhodamine, methyl ester (TMRM) and sorted by fluorescence-activated cell sorting as previously re-

ported [10]. The collected cells, stained for the cardiac-specific  $\alpha$ -actinin and reanalyzed by flow cytometry, reached approximately 60% enrichment for cardiomyocytes (supplemental online Fig. 3). In TMRM-sorted cells, expression of three fetal genes was significantly augmented in TG compared with NTG-enriched iCMs (Fig. 4D), indicating the activation of hypertrophic genetic program in vitro.

## DISCUSSION

R120G cardiomyopathy, a myofibrillar disorder, is well-characterized by the formation of aggregates and the hypertrophic response [2–4]. Although iPSC-derived iCMs have recapitulated several arrhythmogenic diseases and dilated cardiomyopathy [9, 11, 12], none of the characteristics of R120G syndrome has yet been reproduced by this stem cell in vitro differentiation technology.

As transgene expression is known to exhibit mosaic expression, which is likely related to epigenetic mechanisms [13], we found that CryAB immunostaining revealed similar heterogeneity between R120G CryAB TG iCMs with high and low levels of expression, recapitulating what was previously and independently described in the corresponding mouse models [3, 4]. The

present studies also have established that the induction of cardiac hypertrophy closely correlated with the amount of misfolded protein expression. Cellular hypertrophy, however, has not been universally observed as reported in LEOPARD patient-specific iCMs [7] but not from patients with dilated cardiomyopathy [12], indicating that our model brings new insight into the ability of iCMs to recapitulate human cardiac hypertrophy features.

In transgenic mouse cardiomyocytes, R120GCryAB protein accumulates in large aggregates, whereas we observed that TG iCM aggregates were much smaller and more dispersed [3], suggesting important physiological and environmental differences between adult cardiomyocytes *in vivo* and iPSC-derived cardiomyocytes *in vitro*. Several laboratories have observed that iCMs do not reach the full state of terminal differentiation and maturity found in the adult heart [14]. Nevertheless, both aggregate formation and cell size change were observed in iCMs identified by cTnT immunodetection, which implies that the cell lineage had progressed enough in cardiac differentiation program to express this marker [15].

## CONCLUSION

*In vitro* production of unlimited numbers of cardiomyocytes has incalculable advantages, and our study has validated the use of iPSCs to model misfolded CryAB protein-related diseases. Ongoing projects in our laboratory are establishing a patient-specific iPSC model containing CryAB mutations. Our model could provide a clear step forward by permitting analysis in a disease-specific system *in vitro*.

## ACKNOWLEDGMENTS

We are grateful for expert technical assistance from and discussion with our colleagues at the Gladstone Stem Cell Core Facility, J. Arnold, T. Nguyen, S. Banerjee Mustafi, and T. Kanai. This work was supported by 2R01-HL063834-06, 5R01-HL074370-03, and NIH 5DP1OD006438-03 (to I.J.B.) and by an American Heart Association postdoctoral fellowship (12POST9700016) to P.L.

## AUTHOR CONTRIBUTIONS

P.L. and H.Z.: conception and design, collection and assembly of data, data analysis and interpretation, manuscript writing, final approval of manuscript; E.C.: collection and assembly of data, data analysis and interpretation, manuscript writing, final approval of manuscript; Q.L. and G.T.: collection and assembly of data; M.R. and K.M.: data analysis and interpretation, manuscript writing; K.I.: data analysis and interpretation, manuscript writing, final approval of manuscript, iPSC training; P.C.: data analysis and interpretation, cardiomyocyte differentiation training; D.W.: data analysis and interpretation; D.S.: data analysis and interpretation, iPSC training; I.B.: financial support, data analysis and interpretation, manuscript writing, final approval of manuscript.

## DISCLOSURE OF POTENTIAL CONFLICTS OF INTEREST

D.S. is a compensated scientific advisory board member of RegenerX and iPierian.

## REFERENCES

- Jakob U, Gaestel M, Engel K et al. Small heat shock proteins are molecular chaperones. *J Biol Chem* 1993;268:1517–1520.
- Vicart P, Caron A, Guicheney P et al. A missense mutation in the alphaB-crystallin chaperone gene causes a desmin-related myopathy. *Nat Genet* 1998;20:92–95.
- Wang X, Osinska H, Klevitsky R et al. Expression of R120G-alphaB-crystallin causes aberrant desmin and alphaB-crystallin aggregation and cardiomyopathy in mice. *Circ Res* 2001;89:84–91.
- Rajasekaran NS, Connell P, Christians ES et al. Human alpha B-crystallin mutation causes oxido-reductive stress and protein aggregation cardiomyopathy in mice. *Cell* 2007;130:427–439.
- Bova MP, Yaron O, Huang Q et al. Mutation R120G in alphaB-crystallin, which is linked to a desmin-related myopathy, results in an irregular structure and defective chaperone-like function. *Proc Natl Acad Sci USA* 1999;96:6137–6142.
- Maloyan A, Gulick J, Glabe CG et al. Exercise reverses preamyloid oligomer and prolongs survival in alphaB-crystallin-based desmin-related cardiomyopathy. *Proc Natl Acad Sci USA* 2007;104:5995–6000.
- Carvajal-Vergara X, Sevilla A, D'Souza SL et al. Patient-specific induced pluripotent stem-cell-derived models of LEOPARD syndrome. *Nature* 2010;465:808–812.
- Malan D, Friedrichs S, Fleischmann BK et al. Cardiomyocytes obtained from induced pluripotent stem cells with long-QT syndrome 3 recapitulate typical disease-specific features *in vitro*. *Circ Res* 2011;109:841–847.
- Moretti A, Bellin M, Welling A et al. Patient-specific induced pluripotent stem-cell models for long-QT syndrome. *N Engl J Med* 2010;363:1397–1409.
- Hattori F, Chen H, Yamashita H et al. Nongenetic method for purifying stem cell-derived cardiomyocytes. *Nat Methods* 2010;7:61–66.
- Yazawa M, Hsueh B, Jia X et al. Using induced pluripotent stem cells to investigate cardiac phenotypes in Timothy syndrome. *Nature* 2011;471:230–234.
- Sun N, Yazawa M, Liu J et al. Patient-specific induced pluripotent stem cells as a model for familial dilated cardiomyopathy. *Sci Transl Med* 2012;4:130–147.
- Krepulat F, Lohler J, Heinlein C et al. Epigenetic mechanisms affect mutant p53 transgene expression in WAP-mutp53 transgenic mice. *Oncogene* 2005;24:4645–4659.
- Laflamme MA, Murry CE. Heart regeneration. *Nature* 2011;473:326–335.
- Boheler KR, Czyz J, Tweedie D et al. Differentiation of pluripotent embryonic stem cells into cardiomyocytes. *Circ Res* 2002;91:189–201.



See [www.StemCellsTM.com](http://www.StemCellsTM.com) for supporting information available online.